communications physics

Article

https://doi.org/10.1038/s42005-024-01595-9

Exceptional classifications of non-Hermitian systems

Check for updates

Jung-Wan Ryu [1,5], Jae-Ho Han [1,5], Chang-Hwan Yi[1], Moon Jip Park[2,3,6] ✉ & Hee Chul Park [4,6] ✉

Eigenstate coalescence in non-Hermitian systems is widely observed in diverse scientific domains encompassing optics and open quantum systems. Recent investigations have revealed that adiabatic encircling of exceptional points (EPs) leads to a nontrivial Berry phase in addition to an exchange of eigenstates. Based on these phenomena, we propose in this work an exhaustive classification framework for EPs in non-Hermitian physical systems. In contrast to previous classifications that only incorporate the eigenstate exchange effect, our proposed classification gives rise to finer $\mathbb{Z}_2$ classifications depending on the presence of a π Berry phase after the encircling of the EPs. Moreover, by mapping arbitrary one-dimensional systems to the adiabatic encircling of EPs, we can classify one-dimensional non-Hermitian systems characterized by topological phase transitions involving EPs. Applying our exceptional classification to various multiband systems, we expect to enhance the understanding of topological phases in non-Hermitian systems.

Non-Hermitian physical systems exhibit a unique type of singularity, known as exceptional points (EPs), where distinct eigenstates of the Hamiltonian coalesce with each other[1–7]. EPs have garnered significant interest due to their potential applications in diverse fields such as optics, acoustics, and open quantum systems[8–15]. As a system undergoes an adiabatic deformation that encircles an EP or EPs, the eigenstates exchange in a nontrivial manner. This eigenstate switching effect allows for the classification of EPs based on the conjugacy class of the permutation group[16].

Concurrently, the study of Hermitian topological phases has focused on the classification of topological invariants associated with the Berry phase[17–20]. The quantized Zak phases in the Su–Schrieffer–Heeger (SSH) model are one representative example[21–26]. In EPs, the wave functions can accompany an additional geometric (Berry) phase shift of π after the encircling of an EP. This connection between EPs and nontrivial Berry phases has been both theoretically and experimentally explored[27–31] and suggests a more complex structure for EPs. As we show below, these two seemingly unrelated phenomena—namely the nontrivial Berry phase and EPs—are intimately tied together.

In this work, we demonstrate that the EPs are characterized by *exceptional classifications*, a scheme we propose to incorporate the information of both eigenstate switching and the additional Berry phase. The entangled relation between the state switching and additional Berry phase makes constraints of topological invariants. In addition, by viewing one-dimensional (1D) systems as adiabatic deformations encircling EPs, we achieve a full characterization of 1D non-Hermitian topological systems. This characteristic reveals topological phase transitions between different phases, where the phase transitions accompany the EPs. Our identification of this exceptional class lays the groundwork for further exploration of the rich physics of non-Hermitian systems.

Results

Classification scheme

We consider a general N-state non-Hermitian system with two external parameters. When encircling the system's EPs through adiabatic deformation, the eigenstates exhibit the exchange effect, which can be represented by a permutation of the N states[32,33]. The cyclic structure of such permutations can be formally mapped by the conjugacy class $[\sigma]$ (with representative permutation σ), which forms a product of cycles. Specifically, we can use the following notation to represent the permutation properties of the EPs, as in[16,34]:

$$[\sigma] = 1^{n_1} 2^{n_2} \cdots N^{n_N}, \quad \sum_{q=1}^{N} q n_q = N. \tag{1}$$

[1]Center for Theoretical Physics of Complex Systems, Institute for Basic Science (IBS), Daejeon, Republic of Korea. [2]Department of Physics, Hanyang University, Seoul, Republic of Korea. [3]Research Institute for Natural Science, Hanyang University, Seoul, Korea. [4]Department of Physics, Pukyong National University, Busan, Republic of Korea. [5]These authors contributed equally: Jung-Wan Ryu, Jae-Ho Han.[6]These authors jointly supervised this work: Moon Jip Park, Hee Chul Park. ✉e-mail: moonjippark@hanyang.ac.kr; hc2725@gmail.com

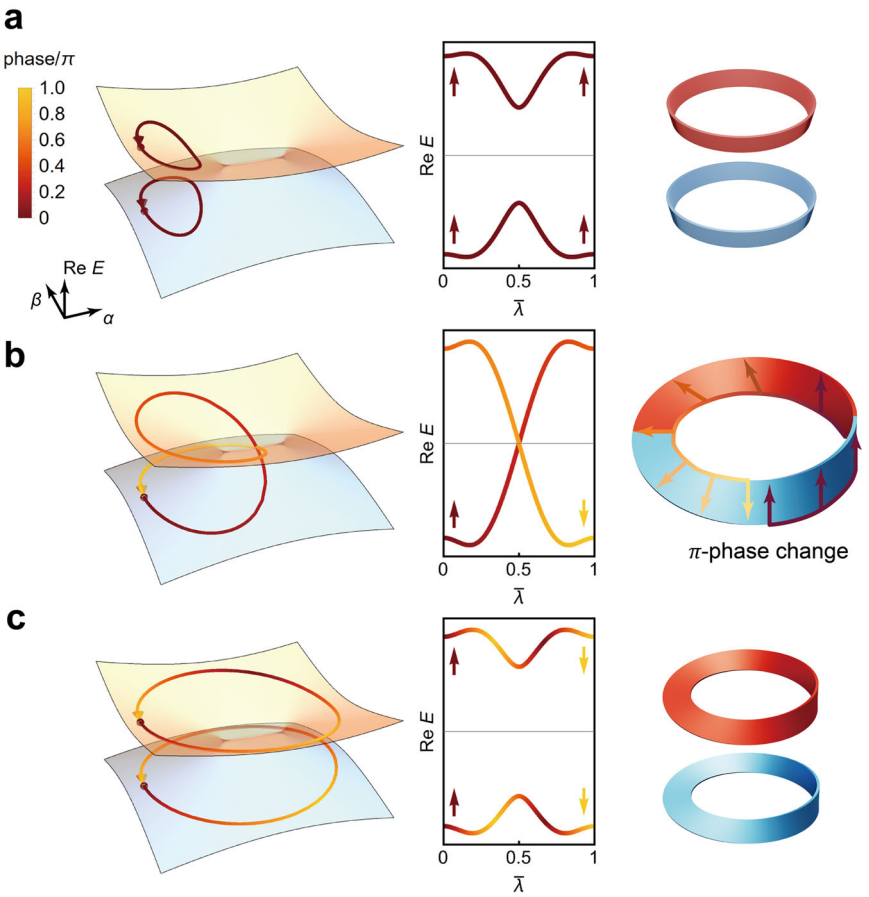

Fig. 1 | Illustration of the switching effect and Berry phase after an encircling of Exceptional Points (EPs) in parameter space. The figures depict the evolution of the topological winding on the real energy band across parameter space (α, β), as indicated by the Berry phase color bar on each energy band (see Supplementary Note 2). Each set consists of three representations: (i) a parameter space mapping, (ii) an unfolded band structure, and (iii) a corresponding schematic of a strip. The color coding within each figure notes the energy band index, with the normal strip symbolizing a trivial phase and the Möbius strip symbolizing a non-trivial phase. For **a** No encircling of EPs results in no state switching, indicating a zero phase change and a trivial topology. For **b** Encircling one EP leads to state switching, denoted by a π phase change, signifying a non-trivial topology. For **c** Encircling two EPs, despite no state switching, results in a π phase change due to the cumulative topological impact.

Each cycle is represented in the form c^{n_c}, where c indicates the cycle length (number of encirclings required to return to the initial state), and the superscript $n_c \in \{0, 1, \cdots, N\}$ denotes the number of c-cycles in $[\sigma]$. For instance, in a two-state system, there exist two possible exchanges of eigenstates after the encircling of adiabatic deformations, represented by the conjugacy classes $[e] = 1^2$, $[\sigma] = 2^1$, where e represents the identity permutation and σ denotes a transposition.

Furthermore, in addition to the conjugate classification there exist Berry phases of the wave functions. The complex Berry phase[35–38] can be defined as

$$\gamma = i \oint_{\mathscr{C}} \frac{<\phi(\lambda)|\partial_\lambda \psi(\lambda)>}{<\phi(\lambda)|\psi(\lambda)>} d\lambda. \tag{2}$$

Here, $\mathscr{C}$ is a closed path in $\mathscr{M} \times \mathbb{C}$ where $\mathscr{M}$ is the parameter space and $\mathbb{C}$ is the complex number space, λ is a parameterization of the path $\mathscr{C}$, and ϕ and ψ respectively are the left and right eigenstates of the Hamiltonian $H(\lambda)$. Due to the complex nature of the energy of non-Hermitian Hamiltonians, we will concentrate on a two-dimensional parameter space (or, codimension two). Since the double encircling of a single EP in parameter space induces a nontrivial π Berry phase for the states (see Methods and Supplementary Note 1), the conjugate classifications of the EPs are further sub-classified depending on the presence of the Berry phase. We refer to these finer classifications of the conjugacy class as the *exceptional class*. In the following discussion, we use the notation $\bar{c}$ for the c-cycles with π Berry phases.

A constraint arises from the consistency between the switching effect and the Berry phase: the sum of the Berry phases of the cycles in the conjugacy classes should be 0 and π for even and odd permutations, respectively[31]. Note that the parity of permutations remains invariant under conjugation. As an example, consider a two-state system having two conjugacy classes, $[e] = 1^2$, $[\sigma] = 2^1$. Under the consistency constraint, the exceptional classes are

$$[e] = 1^2, \bar{1}^2, \quad [\sigma] = \bar{2}^1, \tag{3}$$

where the sums of the Berry phases for all bands are 0 (mod 2π) for 1^2 and $\bar{1}^2$, and π for $\bar{2}^1$. This is consistent with the parities of e (even) and σ (odd). The switching effect and the Berry phases for 1^2, $\bar{2}^1$, and $\bar{1}^2$ cases are illustrated by in Fig. 1a–c, respectively. Note that $\bar{1}^2$ can only appear in systems with multiple EPs. This classification scheme can be generalized to N-state systems. Using signed holonomy matrices, the classes can be obtained systematically. We note that some conjugacy classes are connected by gauge transformation and should be identified; details are in Methods and Section II of SI.

Non-reciprocal SSH model

In the following, we apply the exceptional classification framework to 1D systems. As an example, we consider the non-reciprocal Su–Schrieffer–Heeger (SSH) model[39–43], where the Hamiltonian is given as

$$H = \sum_i t e^{\theta} a_{i+1}^\dagger b_i + t e^{-\theta} b_{i-1}^\dagger a_i + d a_i^\dagger b_i + d b_i^\dagger a_i. \tag{4}$$

Here, d represents intra-unit-cell hopping, t denotes inter-unit-cell hopping, and θ describes the non-reciprocity between left and right directional hopping [Fig. 2a]. The energy is measured in d, or $d = 1$. It is noted that our classification scheme based on the EPs in general non-Hermitian systems does not require any symmetry constraints since the additional Berry phase after encircling EPs is always quantized without consideration of symmetry. When we apply our classification scheme to one-dimensional lattice models, the topological invariant associate with Berry phases is Zak phases, which can be quantized only when the Hamiltonian possesses additional symmetries. In the above non-

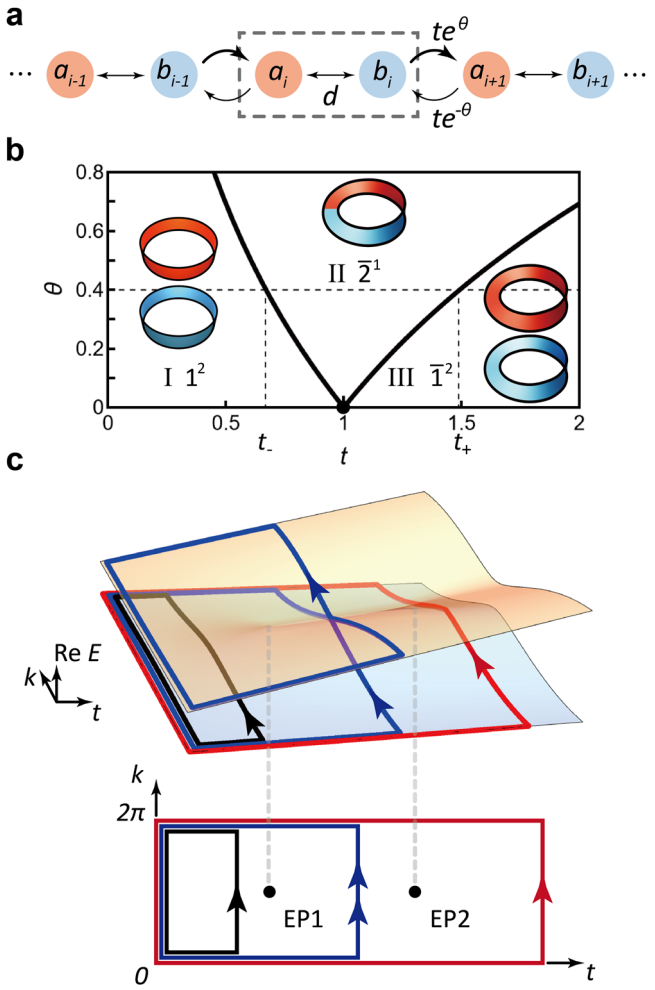

Fig. 2 | Two-band Su-Schrieffer-Heeger (SSH) model. a Non-Hermitian SSH model with non-reciprocal inter-unit-cell hopping. Intra-unit-cell hoppings are d and inter-unit-cell hoppings are te^{θ} and $te^{-\theta}$. The dashed box denotes the unit cell. **b** Phase diagrams of the non-Hermitian SSH model. The black dot denotes a Dirac point, and the curved lines denote EPs. The 1^2 regime (I) is a trivial line-gapped regime of two trivial 1-cycle bands, the $\bar{2}^1$ regime (II) is a point-gapped regime of a 2-cycle non-separable band with a π Zak phase, and the $\bar{1}^2$ regime (III) is a line-gapped regime of two 1-cycle bands with π Zak phases. **c** The connection between the Zak phase of the one-dimensional SSH model and the EPs in parameter space, (t,k) space. Black, blue, and red paths respectively contain zero, one, and two EPs in (t,k) space, which correspond to 1^2, $\bar{2}^1$, and $\bar{1}^2$ phases.

reciprocal SSH model, it is known that the Zak phase is quantized in the units of π because of chiral symmetry[42,44].

We observe three distinct topological phases, where each phase corresponds to adiabatic deformations with different exceptional classifications. Circular strips in Fig. 2b represent the corresponding band structure in the complex energy plane. While each complex energy band forms a closed loop in the complex energy space, we observe that the total number of non-separable energy bands varies from a single band (phase II) with a point gap to two bands separated by a line gap (phase I, III)[45,46]. The spectral flow as a function of momentum shows that the bands in phases I and III form a 2π periodicity (1-cycle band, $[e]$). In contrast, the bands in phase II form a 4π periodic spectral flow (2-cycle band, $[\sigma]$) due to the eigenstate switching effect. These are represented schematically in Fig. 2b, where the red and blue strips in phases I and III appear as two separated bands, whereas the strip with both red and blue parts in phase II appears as a connected band.

In addition, the two 1-cycle bands in phases I and III are further distinguished by the presence of a nontrivial Zak phase[42–44]. The bands in phase I (III) have a Zak phase of $\theta = 0(\pi)$, which indicates that the bands

Table 1 | Properties of phases for the two-band system

Phases (class)	Phase I (1^2)	Phase II ($\bar{2}^1$)	Phase III ($\bar{1}^2$)
(i) Number of separated bands	2	1	2
(ii) Order of cycles	(1,1)	2	(1,1)
(iii) Berry phases	(0,0)	π	(π,π)
(iv) Connection to Hermitian	O	X	O

(i) number of separated bands, (ii) order of cycles for each band, (iii) Berry phases of each separated band, and (iv) whether the phases are connected to Hermitian systems without phase transition represented by O or X.

belong to the classification 1 ($\bar{1}$). The nontrivial π Zak phase doubles the periodicity of the spectral flow, resulting in a 4π periodic spectral flow, as schematically represented by the twisted strips in phase III of Fig. 2b.

The topological phase transitions between each exceptional class can be understood by viewing the Bloch Hamiltonian as an adiabatic encircling of the EPs in two-dimensional parameter space (t,k), as shown in Fig. 2c. In the Hermitian limit ($\theta = 0$), a single Dirac point occurs at $(t,k) = (d,\pi)$. The presence of non-reciprocity splits the Dirac point into a pair of EPs at $(t,k) = (de^{\pm\theta},\pi)$. Within this parameter space, the three topological phases correspond to three distinct loops of the spectral flow that contain zero, one, and two EPs, respectively [Fig. 2**c**]. As a result, the adiabatic encircling at the phase transitions must touch the EPs. The phase transitions between distinct exceptional classes accompany the EPs in the energy spectra [see Fig. 2b].

For phase I where $t < t_-$, the black loop in Fig.2**c** contains no EP. Correspondingly, each state returns to its initial state after a single loop in the parameter space, consistent with the trivial Zak phase. Thus, systems in phase I is identified as class 1^2. For phase II where $t_- < t < t_+$, the presence of an EP within the blue loop, a switching of states under spectral flow with an additional π Zak phase. Accordingly, phase II is identified as $\bar{2}^1$. Finally, for phase III where $t > t_+$, the red loop encloses a pair of EPs that results in the states returning to their initial state after a single encircling, and each state has a Zak phase of π. Thus phase III is identified as class $\bar{1}^2$. Based on the classification scheme introduced in the previous section, this model exhausts all possible classes of two-state systems. Furthermore, when $t > t_+$, there is no switching of states as the loop encircles the two EPs, but the π Zak phase is retained, which distinguishes phase III ($\bar{1}^2$ class) from phase I (1^2 class). As a result, our model exhausts all possible exceptional classes of 1D two-band systems. Properties of phases for the two-band system are summarized in Table 1.

Application to generic systems

To illustrate the general applicability of our classification, we now consider three-band systems. According to our classification (Supplementary Table S1 in Supplementary Note 2), there exist five exceptional classes as follows,

$$[e] = 1^3,\ 1^1\bar{1}^2,\ [\sigma] = \bar{1}^1 2^1,\ 1^1\bar{2}^1,\ [\tau] = 3^1. \tag{5}$$

Our proposed 1D three-band model, which realizes all possible exceptional classes, has the following Bloch Hamiltonian [see Fig. 3a for the real-space structure]:

$$h(k) = \begin{pmatrix} 0 & d_1 & d_2 + te^{\theta}e^{-ik} \\ d_1 & 0 & d_1 \\ d_2 + te^{-\theta}e^{ik} & d_1 & 0 \end{pmatrix}. \tag{6}$$

The corresponding phase diagram is depicted as a function of t and θ in Fig. 3b. In the Hermitian limit ($\theta = 0$), two Dirac points occur, where one Dirac point corresponds to the band touching between the second and third bands and the other to the first and second bands, respectively. As non-

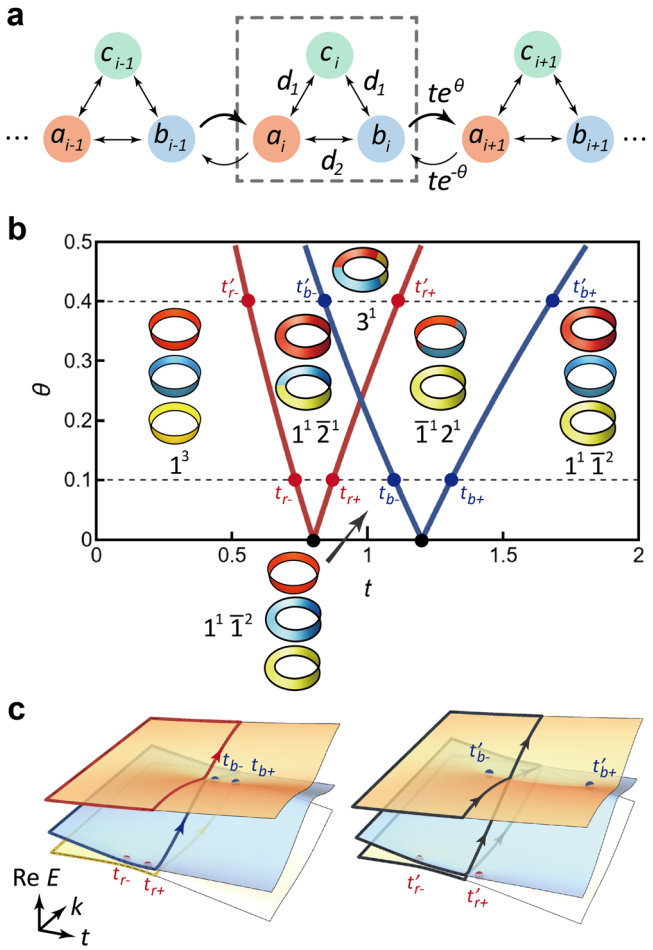

Fig. 3 | Three-band SSH model. a Non-Hermitian three-band model illustrating non-reciprocal inter-unit-cell hopping with intra-unit-cell hoppings d_1 and d_2, and inter-unit-cell hoppings te^{θ} and $te^{-\theta}$. The dashed box highlights the unit cell. **b** Phase diagrams of the Hamiltonian (Eq. (6)) on the (t, θ) plane for $d_1 = 1.0$ and $d_2 = 0.2$. Black dots signify Dirac points. Red and blue lines indicate two pairs of EPs associated with the second and third bands, and with the first and second bands, respectively. In the Hermitian limit ($\theta = 0$), two phases, 1^3 and $1^1\bar{1}^2$, are present; for the non-Hermitian case ($\theta \neq 0$), five phases, 1^3, $1^1\bar{1}^2$, $1^1\bar{2}^1$, $\bar{1}^1 2^1$, and 3^1, are distinguished by the boundaries formed by pairs of EPs. The strips' colors (Yellow, Blue, and Red) correspond to the energy band index (1st, 2nd, and 3rd). **c** Real energy surfaces at $\theta = 0.1$ (left) and $\theta = 0.4$ (right) in the parameter space (t, k), with paths along the Brillouin zone ($k \in [0, 2\pi]$) and $t = 0, 1$. EPs are marked by red and blue dots, related to the EPs shown in **b**. The $1^1\bar{1}^2$ phase includes three separate paths; blue and yellow paths encompass two EPs each, resulting in a π phase change. In the 3^1 phase, a single 3-cycle band path encircles two EPs, and three loops result in zero phase change.

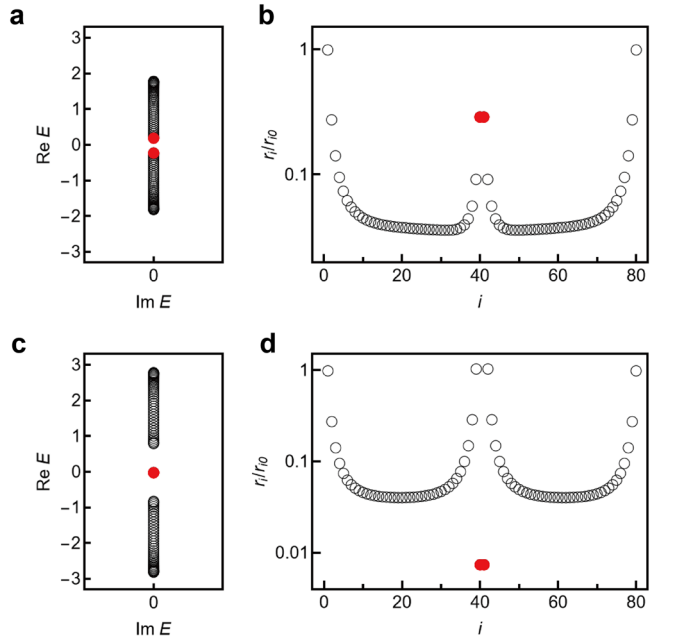

Fig. 4 | Edge states and EP. a, **b** Complex energy spectra and **c**, **d** phase rigidities of the eigenstates for the non-Hermitian SSH model under open boundary conditions. **a**, **c** are in the trivial phase, $t = 0.8 < t_c = 1$, while **b**, **d** are in the nontrivial phase, $t = 1.6 > t_c$ with $\theta = 0.4$. The total number of lattice sites is $2N = 80$, and the eigenstates are labeled in increasing order of energy. The red dots are Nth and $(N+1)$th states, which are the states nearest to the gap in the trivial phase and the edge states in the nontrivial phase.

reciprocity is turned on ($\theta \neq 0$), each Dirac point is split into a pair of EPs (total four EPs), each of which corresponds to a phase transition point in (t, k) space.

First, we consider the case of $\theta = 0.1$. The energy band structures are shown as schematic figures in the inset of Fig. 3b. When $t < t_{r-}$, there are three 1-cycle bands with zero Zak phases. When $t_{r-} < t < t_{r+}$, the second and third bands are not separable, while the first band is separable. The non-separable 2-cycle bands have a π Zak phase, and the separable 1-cycle band has a zero Zak phase. When $t_{r+} < t < t_{b-}$, the three bands are fully separated. The second and third bands have π Zak phases, but the first band has a zero Zak phase. When $t_{b-} < t < t_{b+}$, the sum of the Zak phases of the first and second bands changes from π to 0 at $t = t_{b-}$. The first and second bands are not separable. When $t > t_{b+}$, the three bands are fully separated. The first and third bands have π Zak phases, but the second band has a zero Zak phase.

Next, we consider the case of $\theta = 0.4$. When $t'_{b-} < t < t'_{r+}$, the three bands are not separated and the Zak phase of the non-separable 3-cycle band is zero. In Fig. 3c, the real band structures are shown for two different phases, $t_{r+} < t < t_{b-}$ for $\theta = 0.1$ (left) and $t'_{b-} < t < t'_{r+}$ for $\theta = 0.4$ (right). The topological phases of the band structures are the same as the case of $\theta = 0.1$ in the other regimes. The phase transitions at the EPs are equivalent to adding or removing an EP from the closed loop around the EPs following the adiabatic encircling. The different topological phases result from the positions as well as the number of the EPs in the space (t, k). In summary, the phases are identified as the classes 1^3, $1^1\bar{2}^1$, $1^1\bar{1}^2$, $\bar{1}^1 2^1$, $1^1\bar{1}^2$, and 3^1, as shown in Fig. 3b. Thus the model exhausts all possible classes of three-state systems.

Edge states at EPs under open boundary conditions

The nontrivial Zak phase manifests as a well-defined topological boundary mode even in non-Hermitian systems. Such boundary modes are distinguished from Hermitian topological boundary modes as the phase transition of the topological phase is manifested by a single EP rather than by a Dirac point.

In the open boundary condition, the non-Hermitian SSH model exhibits two energy continuums separated by a gap where the gap closes at $t = t_c = 1$, signifying a phase transition. See Fig. 4a, b. For $t > t_c$ (nontrivial phase), mid-gap states emerge [red dots in Fig. 4b] as a consequence of the nontrivial Zak phase. It is noteworthy that in the Hermitian limit, $\theta = 0$, these states correspond to edge states. Figure 4c, d display the phase rigidities of the states, $r_i = \langle\phi_i|\psi_i\rangle / \sqrt{\langle\phi_i|\phi_i\rangle\langle\psi_i|\psi_i\rangle}$, where ϕ_i and ψ_i are left and right eigenstates, respectively, and i is the index of the states[47,48]. The mid-gap states are edge states, and their phase rigidities are significantly smaller. This implies that the edge states are much closer to the EP, which is consistent with the phase transition line at $t = 1$.

Discussion

Our system formally belongs to A class which has $\mathbb{Z}$-class point gap topology. The winding number of the point-gapped phases in non-

Hermitian systems can explain the symmetry-protected skin effect since the invariants physically correspond to the winding numbers of complex eigenvalues of Hamiltonians. However, the winding number does not explain the Zak phase associated with the EP. Homotopical framework towards the topological classification of non-Hermitian systems with separable and non-separable band structures enables us to see more topological invariants beyond K-theoretical approaches[49–59].

In conclusion, we have introduced a classification scheme for 1D non-Hermitian topological phases based on exceptional classes. The approach combines the information of both eigenstate switching and the additional Zak phase. We demonstrated the applicability of this classification to both two-band and three-band systems, revealing the rich structure of non-Hermitian topological phases and the interplay between exceptional points and topological properties. The more examples are presented in Supplementary Note 3. We expect that our classification scheme can be applied to other non-Hermitian systems and utilized to reveal the structure of intertwined topological and non-Hermitian properties. The encircling an EP have been implemented as the wave propagations in the optical waveguides, where many abnormal and interesting phenomena related to the state switching have been reported[4,60–62]. We also expect that additional interference phenomena can be demonstrated due to the additional Berry phase during encircling EPs realized as wave propagations in optical waveguides.

Methods

Berry phase in non-Hermitian systems

The two features of Non-Hermitian systems are (i) non-orthonormality of eigenstates of Hamiltonian and (ii) Riemann surface structure of complex energy in parameter space, or exchanging of states. To incorporate these properties, the Berry phase is generalized as follows: (i) use both left- and right-eigenstates (ii) multiple encircling in the parameter space [Eq. (2)]. As an illustration, consider a two-state Hamiltonian

$$H=\begin{pmatrix}0 & 1\\ z & 0\end{pmatrix},\quad z=x+iy,\quad x,y\in R. \tag{7}$$

If $z=0$, the Hamiltonian is in a Jordan canonical form that represents the EP, and z is considered as a perturbation near the EP. The right eigenvalues and right eigenstates (up to normalization) of H are

$$H|v_\pm\rangle=E_\pm|v_\pm\rangle,\quad E_\pm=\pm\sqrt{r}e^{i\frac{\theta}{2}},\quad |v_\pm\rangle=\begin{pmatrix}\pm\frac{1}{\sqrt{r}}e^{-i\frac{\theta}{2}}\\ 1\end{pmatrix}. \tag{8}$$

Corresponding left eigenvectors are

$$\langle u_\pm|H=E_\pm\langle u_\pm|,\quad \langle u_\pm|=\begin{pmatrix}\pm\sqrt{r}e^{i\frac{\theta}{2}} & 1\end{pmatrix}, \tag{9}$$

The right- and left-eigenstates form a biorthogonal basis.

Now consider a circular path $\mathscr{C}$ of radius R around an EP that is centered at the origin of the z-plane. Reflecting the Riemann surface of eigenstates, the path winds around the EP twice:

$$\mathscr{C}:\lambda\mapsto z=Re^{i\lambda},\quad \lambda\in[0,4\pi]. \tag{10}$$

During the encircling, the following instantaneous eigenstates are used:

$$|v_\pm(\lambda)\rangle=\begin{pmatrix}\pm\frac{1}{\sqrt{R}}e^{-i\frac{\lambda}{2}}\\ 1\end{pmatrix},\quad \langle u_\pm(\lambda)|=\begin{pmatrix}\pm\sqrt{R}e^{i\frac{\lambda}{2}} & 1\end{pmatrix}. \tag{11}$$

Then the Berry phase along this path $\mathscr{C}$ is given by

$$\gamma_\pm(\mathscr{C})=\int_0^{4\pi}d\lambda\,\frac{i\langle u_\pm(\lambda)|\partial_\lambda|v_\pm(\lambda)\rangle}{\langle u_\pm(\lambda)||v_\pm(\lambda)\rangle}=\int_0^{4\pi}d\lambda\,\frac{1}{4}=\pi. \tag{12}$$

Note that the phase is topological since it depends on the winding number of EP (up to 2π) but not on the geometry of the path.

Signed holonomy matrices

The exchange of states after the encircling EPs in the parameter space of the Hamiltonian can be conveniently represented by using holonomy matrices. Consider the above two-state Hamiltonian H. Starting at $z=1$ and after encircling the EP (z=0) once, the states exchange:

$$\begin{pmatrix}v_+\\ v_-\end{pmatrix}\mapsto\begin{pmatrix}v_-\\ v_+\end{pmatrix}=\mathscr{M}\begin{pmatrix}v_+\\ v_-\end{pmatrix},\quad \mathscr{M}=\begin{pmatrix}0 & 1\\ 1 & 0\end{pmatrix}, \tag{13}$$

where $v_\pm=(\pm1,1)^T$ are eigenstates at $z=1$. The matrix $\mathscr{M}$ is the holonomy matrix.

To incorporate the π Berry phase after encircling the EP twice, we introduce signed holonomy matrices. In the two-band example,

$$\mathscr{M}=\begin{pmatrix}0 & 1\\ 1 & 0\end{pmatrix}\to\mathscr{M}_s=\begin{pmatrix}0 & 1\\ -1 & 0\end{pmatrix}. \tag{14}$$

Then one can construct conjugate classes of the group generated by the signed holonomy matrices. However, there are physically equivalent classes in this classification because some holonomy matrices can be connected by the gauge transformation. For example, consider the two holonomy matrices

$$\mathscr{M}_{s1}=\begin{pmatrix}0 & 1\\ -1 & 0\end{pmatrix},\quad \mathscr{M}_{s2}=\begin{pmatrix}0 & -1\\ 1 & 0\end{pmatrix}. \tag{15}$$

These holonomy matrices describe processes

$$\mathscr{M}_{s1}:\begin{cases}v_+\to -v_-\to -v_+\\ v_-\to v_+\to -v_-\end{cases},\quad \mathscr{M}_{s2}:\begin{cases}v_+\to v_-\to -v_+\\ v_-\to -v_+\to -v_-\end{cases}, \tag{16}$$

which can be transformed into each other by a gauge transformation. Identifying these classes leads to the classification described in the main text.

Data availability

All the calculation details are provided in Supplementary Information.

Received: 3 July 2023; Accepted: 11 March 2024;
Published online: 28 March 2024

References

1. Kato, T. Perturbation theory of linear operators. (Springer, Berlin, 1966).
2. Heiss, W. D. & Sannino, A. L. Avoided level crossing and exceptional points. *J. Phys. A* **23**, 1167–1178 (1990).
3. Heiss, W. D. Exceptional points of non-Hermitian operators. *J. Phys. A* **37**, 2455–2464 (2004).
4. Doppler, J. et al. Dynamically encircling an exceptional point for asymmetric mode switching. *Nat. (Lond.)* **537**, 76 (2016).
5. Chen, H.-Z. et al. Revealing the missing dimension at an exceptional point. *Nat. Phys.* **16**, 571 (2020).
6. Tang, W. et al. Exceptional nexus with a hybrid topological invariant. *Science* **370**, 1077 (2020).
7. Yang, Z., Schnyder, A. P., Hu, J. & Chiu, C.-K. Fermion doubling theorems in two-dimensional non-Hermitian systems for fermi points and exceptional points. *Phys. Rev. Lett.* **126**, 086401 (2021).
8. Xu, H., Mason, D., Jiang, L. & Harries, J. G. E. Topological energy transfer in an optomechanical system with exceptional points. *Nat. (Lond.)* **537**, 80 (2016).
9. Shi, C. et al. Accessing the exceptional points of parity-time symmetric acoustics. *Nat. Commun.* **7**, 11110 (2016).

10. Miao, P. et al. Orbital angular momentum microlaser. *Science* **353**, 464 (2016).
11. Ding, K., Ma, G., Xiao, M., Zhang, Z. Q. & Chan, C. T. Emergence, coalescence, and topological properties of multiple exceptional points and their experimental realization. *Phys. Rev. X* **6**, 021007 (2016).
12. Chen, W., Özdemir, Ş. K., Zhao, G., Wiersig, J. & Yang, L. Exceptional points enhance sensing in an optical microcavity. *Nat. (Lond.)* **548**, 192 (2017).
13. Yang, H., Wang, C., Yu, T., Cao, Y. & Yan, P. Antiferromagnetism emerging in a ferromagnet with gain. *Phys. Rev. Lett.* **121**, 197201 (2018).
14. Özdemir, Ş. K., Rotter, S., Nori, F. & Yang, L. Parity-time symmetry and exceptional points in photonics. *Nat. Mater.* **18**, 783 (2019).
15. Miri, M.-A. & Alù, A. Exceptional points in optics and photonics. *Science* **363**, eaar7709 (2019).
16. Ryu, J. W., Han, J. H. & Yi, C.-H. Classification of multiple arbitrary-order non-Hermitian singularities. *Phys. Rev. A* **106**, 012218 (2022).
17. Thouless, D. J., Kohmoto, M., Nightingale, M. P. & den Nijs, M. Quantized Hall Conductance in a Two-Dimensional Periodic Potential. *Phys. Rev. Lett.* **49**, 405 (1982).
18. Sheng, D. N., Balents, L. & Wang, Z. Phase Diagram for Quantum Hall Bilayers at $\nu = 1$. *Phys. Rev. Lett.* **91**, 116802 (2003).
19. Hasan, M. Z. & Kane, C. L. Topological insulators. *Rev. Mod. Phys.* **82**, 3045 (2010).
20. Qi, X.-L. & Zhang, S.-C. Topological insulators and superconductors. *Rev. Mod. Phys.* **83**, 1057 (2011).
21. Su, W. P., Schrieffer, J. R. & Heeger, A. J. Solitons in polyacetylene. *Phys. Rev. Lett.* **42**, 1698 (1979).
22. Asbóth, J. K., Oroszlány, L. & Pályi, A. The Su-Schrieffer-Heeger (SSH) Model, in *A Short Course on Topological Insulators: Band Structure and Edge States in One and Two Dimensions* (Springer International Publishing, Cham, 2016).
23. Zak, J. Berry's phase for energy bands in solids. *Phys. Rev. Lett.* **62**, 2747–2750 (1989).
24. Atala, M. et al. Direct measurement of the Zak phase in topological Bloch bands. *Nat. Phys.* **9**, 795 (2013).
25. Xiao, M., Zhang, Z. Q. & Chan, C. T. Surface impedance and bulk band geometric phases in one- dimensional systems. *Phys. Rev. X* **4**, 021017 (2014).
26. Xiao, M. et al. Geometric phase and band inversion in periodic acoustic systems. *Nat. Phys.* **11**, 240 (2015).
27. Heiss, W. D. Phases of wave functions and level repulsion. *Eur. Phys. J. D.* **7**, 1 (1999).
28. Dembowski, C. et al. Experimental observation of the topological structure of exceptional points. *Phys. Rev. Lett.* **86**, 787 (2001).
29. Dembowski, C. et al. Encircling an exceptional point. *Phys. Rev. E* **69**, 056216 (2004).
30. Gao, T. et al. Observation of non-Hermitian degeneracies in a chaotic exciton-polariton billiard. *Nat. (Lond.)* **526**, 554–558 (2015).
31. Lee, S.-Y., Ryu, J.-W., Kim, S. W. & Chung, Y. Geometric phase around multiple exceptional points. *Phys. Rev. A* **85**, 064103 (2012).
32. Ryu, J.-W., Lee, S.-Y. & Kim, S. W. Analysis of multiple exceptional points related to three interacting eigenmodes in a non-Hermitian Hamiltonian. *Phys. Rev. A* **85**, 042101 (2012).
33. Zhong, Q., Khajavikhan, M., Christodoulides, D. N. & El-Ganainy, R. Winding around non-Hermitian singularities. *Nat. Commun.* **9**, 4808 (2018).
34. Hamermesh, M. *Group Theory and Its Application to Physical Problems*. (Addison-Wesley, New York, 1962).
35. Garrison, J. & Wright, E. Complex geometrical phases for dissipative systems. *Phys. Lett. A* **128**, 177 (1988).
36. Dattoli, G., Mignani, R. & Torre, A. Geometrical phase in the cyclic evolution of non-Hermitian systems. *J. Phys. A: Math. Theor.* **23**, 5795 (1990).
37. Mostafazadeh, A. A new class of adiabatic cyclic states and geometric phases for non-Hermitian Hamiltonians. *Phys. Lett. A* **264**, 11–17 (1999).
38. Liang, S.-D. & Huang, G.-Y. Topological invariance and global Berry phase in non-Hermitian systems. *Phys. Rev. A* **87**, 012118 (2013).
39. Yao, S. & Wang, Z. Edge states and topological invariants of non-Hermitian systems. *Phys. Rev. Lett.* **121**, 086803 (2018).
40. Ghataka, A., Brandenbourgera, M., Wezela, J. V. & Coulaisa, C. Observation of non-Hermitian topology and its bulk-edge correspondence in an active mechanical metamaterial. *Proc. Natl Acad. Sci. USA* **117**, 29561–29568 (2020).
41. Wang, W., Wang, X. & Ma, G. Non-Hermitian morphing of topological modes. *Nat. (Lond.)* **608**, 50–55 (2022).
42. Lieu, S. Topological phases in the non-Hermitian Su-Schrieffer-Heeger model. *Phys. Rev. B* **97**, 045106 (2018).
43. Nehra, R. & Roy, D. Topology of multipartite non-Hermitian one-dimensional systems. *Phys. Rev. B* **105**, 195407 (2022).
44. Vyas, V. M. & Roy, D. Topological aspects of periodically driven non-Hermitian Su-Schrieffer-Heeger model. *Phys. Rev. B* **103**, 075441 (2021).
45. Kawabata, K., Shiozaki, K., Ueda, M. & Sato, M. Symmetry and topology in non-Hermitian physics. *Phys. Rev. X* **9**, 041015 (2019).
46. Kawabata, K., Shiozaki, K., Ueda, M. & Sato, M. Classification of exceptional points and non-hermitian topological semimetals. *Phys. Rev. Lett.* **6**, 066405 (2019).
47. Rotter, I. A non-Hermitian Hamilton operator and the physics of open quantum systems. *J. Phys. A: Math. Theor.* **42**, 153001 (2009).
48. Alvarez, V. M. M., Vargas, J. E. B. & Torres, L. E. F. F. Non-Hermitian robust edge states in one dimension: Anomalous localization and eigenspace condensation at exceptional points. *Phys. Rev. B* **97**, 121401(R) (2018).
49. Li, Z. & Mong, R. S. K. Homotopical characterization of non-Hermitian band structures. *Phys. Rev. B* **103**, 155129 (2021).
50. Wojcik, C. C., Sun, X.-Q., Bzdušek, T. & Fan, S. Homotopy characterization of non-Hermitian Hamiltonians. *Phys. Rev. B* **101**, 205417 (2020).
51. Wang, K., Dutt, A., Wojcik, C. C. & Fan, S. Topological complex-energy braiding of non-Hermitian bands. *Nat. (Lond.)* **598**, 59 (2021).
52. Hu, H. & Zhao, E. Knots and non-hermitian bloch bands. *Phys. Rev. Lett.* **126**, 010401 (2021).
53. Li, L., Mu, S., Lee, C. H. & Gong, J. Quantized classical response from spectral winding topology. *Nat. Commun.* **12**, 5294 (2021).
54. Hu, H., Sun, S. & Chen, S. Knot topology of exceptional point and non-hermitian no-go theorem. *Phys. Rev. Res.* **4**, L022064 (2022).
55. Wojcik, C. C., Wang, K., Dutt, A., Zhong, J. & Fan, S. Eigenvalue topology of non-Hermitian band structures in two and three dimensions. *Phys. Rev. B* **106**, L161401 (2022).
56. Patil, Y. S. S. et al. Measuring the knot of non-Hermitian degeneracies and non-commuting braids. *Nat. (Lond.)* **607**, 271–275 (2022).
57. Zhang, Q. et al. Observation of acoustic non-Hermitian bloch braids and associated topological phase transitions. *Phys. Rev. Lett.* **130**, 017201 (2023).
58. Cartarius, H., Main, J. & Wunner, G. Exceptional points in the spectra of atoms in external fields. *Phys. Rev. A* **79**, 053408 (2009).
59. Demange, G. & Graefe, E.-M. Signatures of three coalescing eigenfunctions. *J. Phys. A: Math. Theor.* **45**, 025303 (2012).
60. Yoon, J. W. et al. Time-asymmetric loop around an exceptional point over the full optical communications band. *Nature* **562**, 86–90 (2018).
61. Zhang, X.-L., Jiang, T. & Chan, C. T. Dynamically encircling an exceptional point in anti-parity-time symmetric systems: asymmetric mode switching for symmetry-broken modes. *Light.: Sci. Appl.* **8**, 88 (2019).
62. Shu, X. et al. Fast encirclement of an exceptional point for highly efficient and compact chiral mode converters. *Nat. Commun.* **13**, 2123 (2022).

Acknowledgements
We acknowledge financial support from the Institute for Basic Science in the Republic of Korea through the project IBS-R024-D1. This research was supported by the National Research Foundation Grant (2021R1A2C109306013). This research was partly supported by the Creation of the quantum information science R&D ecosystem (No. RS-2023-00256050) through the National Research Foundation of Korea (NRF) funded by the Korean government (Ministry of Science and ICT(MSIT)) and by the Pukyong National University Industry-University Cooperation Research Fund in 2023 (No. 202311880001).

Author contributions
The project was conceived by J.-W.R. and J.-H.H. and led by J.-W.R., J.-H.H., and H.C.P. J.-W.R., J.-H.H., C.-H. Yi, and M.J.P. constructed the models and carried out calculations. All authors discussed the results and were involved in preparing the manuscript.

Competing interests
The authors declare no competing interests.

Additional information
Supplementary information The online version contains supplementary material available at https://doi.org/10.1038/s42005-024-01595-9.

Correspondence and requests for materials should be addressed to Moon Jip Park or Hee Chul Park.

Peer review information *Communications Physics* thanks the anonymous reviewers for their contribution to the peer review of this work. A peer review file is available.